ELSEVIER

Polymer 44 (2003) 1469–1480

polymer

www.elsevier.com/locate/polymer

The morphology and mechanical properties of dynamic packing injection molded PP/PS blends

Yong Wang, Yan Xiao, Qin Zhang, Xiao-Ling Gao, Qiang Fu*

Department of Polymer Science and Materials, State Key Laboratory of Polymer Materials Engineering, Sichuan University, Chengdu 610065, People's Republic of China

Received 17 September 2002; received in revised form 18 December 2002; accepted 20 December 2002

Abstract

As a part of long-term project aimed at super polyolefin blends, in this work, we report the mechanical reinforcement and phase morphology of the immiscible blends of polypropylene (PP) and polystyrene (PS) achieved by dynamic packing injection molding (DPIM). The shear stress (achieved by DPIM) and interfacial interaction (obtained by using styrene–butadiene–styrene (SBS) as a compatibilizer) have a great effect on phase morphology thus mechanical properties. The shear-induced morphology with core in the center and oriented zone surrounding the core was observed in the cross-section areas of the samples. The phase inversion was also found to shift towards lower PS content under shear stress, at 70 wt% in the core and 30 wt% in the oriented zone, compared with 80 wt% for static samples (without shear). The tensile strength, tensile modules and impact strength were found largely increase by means of either shear stress or compatibilizer. The PS particle size is greatly reduced with adding of SBS, and the reduced particle size results in greater resistance to deformation, which causes the co-continuous structure at oriented zone change into droplet morphology. The morphology resulting from blending and processing was discussed based on effect of interfacial tension, shear rate, phase viscosity ratio and composition. The observed change of mechanical properties was explained based on the combined effect of phase morphology (droplet-matrix or co-continuous phase) and molecular orientation under shear stress.

Keywords: PP/PS blends; Shear; Morphology

1. Introduction

Polymer blends have been the subject of intense study for a long time, but in the recent years, totally immiscible blends are interesting for many polymer researchers. The typical example for immiscible polymer blends is blend of polypropylene (PP) and polystyrene (PS). PP and PS are two of the most widely used plastics in the world. In this system, one is crystalline phase and the other is amorphous phase. Because the entropy contribution to the Gibbs energy of melt blending is negligible, the immiscible blends from a thermodynamic point of view have some interesting morphology and mechanical properties. For PP/PS blends, many researches were focused on the morphology and mechanical properties [1–7].

Zhimin Xie and others [7] used the Mori–Tanaka model and the Halpin–Tsai model to investigate the moduli and tensile strength of PP/PS blends. They anticipated that there existed a certain minimum volumes fraction ϑ_{min} of dispersed phase. When the volume fraction is less than ϑ_{min}, the ultimate strength will be controlled by matrix deformation, and when the volume fraction of dispersed phase exceeds the minimum value, the ultimate strength will be controlled by the dispersed phase deformation. They also found that PP/PS blend would have a stationary mechanical property in the phase inversion region.

Mitsuyoshi Fujiyama [8] blended PP with 0–30 wt% of three kinds of PS with different melt flow indexes, and found that the degrees of crystallinity and crystalline *c*-axis orientation decreased with PS blending. PS particles were seen the smallest when the ratio of the viscosity of PS to that of PP at molding shear rate was slightly lower that unity. The phase inversion is quite common phenomenon for immiscible polymer blends. The morphology was found to be dependent on the blend composition and the viscosity ration of the constituent components [9–14]. Sung-Goo Lee

* Corresponding author. Fax: +86-28-5405402.
E-mail address: fuqiang1963@yahoo.com (Q. Fu).

0032-3861/03/$ - see front matter © 2003 Elsevier Science Ltd. All rights reserved.
doi:10.1016/S0032-3861(03)00011-9

[10] reported that when the melt viscosity of PS was higher than that of PP, there was a phase inversion at the PS composition of around 75 wt% in PP/PS blends.

Because of the poor interfacial interactions between the immiscible blends from a thermodynamic point of view, many researches focused on the improvement of interfacial interactions. The main method is the use of a suitable modifier that can increase the adhesion and decrease the interfacial tension between the immiscible blends [15–20].

Appleby T. [21] used a commercial triblock co-polymer (Kraton G1652 (SEBS)) as a compatibilizer for PP/PS blends. Their results showed that addition of SEBS greatly improves the impact strength of the blends. D. Hlavata [22–27] and co-workers studied the compatibilizing effect of several co-polymers with styrene and butadiene blocks on PP/PS blends. They found a certain amount of a compatibilizer is localized at the interface between PP and PS. The use of compatibilizer can improve the mechanical properties. Radonjic G. [28] studied the compatibilization of PP/PS with styrene–butadiene–styrene (SBS) and reported that when the content of PP and PS are equal, the co-continuous morphology was observed. The adding of SBS can reduce the diameter of the PS dispersed particles as well as improve the interfacial adhesion between PP and PS phases. They also revealed that SBS was not only located at the interface between PP and PS phases but also formed, together with the pure PS dispersed particles.

Generally, there are three major factors that govern the morphology of immiscible polymer blends. They are: (1) the rheological and interfacial properties of the constituent components (such as, shear viscosity and fluid elasticity, interfacial tension); (2) blend composition; and (3) processing variables (such as temperature, shear rate). In the past, a lot of work has been done on how these three factors determine blend morphology. It is well established that the blend morphology can be grouped roughly into: (1) co-continuous morphology and (2) dispersed morphology. However, it is not clear whether the co-continuous morphology is stable, giving rise to an equilibrium morphology, or an intermediate step that eventually leads to dispersed morphology, and how the external shear stress can affect the final morphology and mechanical properties.

In recent years, dynamic packing injection molding (DPIM) has been found a very important way to control polymer morphology and mechanical properties [29–31]. The main feature of this technology is that the specimen is forced to move repeatedly in the model by two pistons that move reversibly with the same frequency during cooling, which results in preferential orientation of dispersed phase as well as the matrix. We have performed extensive experimental work on the controlling of phase morphology of polyolefin blends, such as PP/LLDPE [32], PP/HDPE [33], PP/EPDM [34,35], HDPE/EVA [36] and PP/clay nanocomposites [37], by using DPIM technique. The super polyolefin blends with high modulus and tensile strength as well as high impact strength has been obtained [32,33,36]. By controlling the EPDM particles as elongated and oriented in PP matrix, a brittle–ductile–brittle transition of impact strength was found for the first as increasing of EPDM content [34,35]. In this work, we extended DPIM technology into PP/PS and PP/PS/SBS blends. Our proposes are two-folds, one is to better understand the morphological development of immiscible polymer blends during external shear stress, and the other is to achieve high performance PP/PS blends by controlling of the orientation, phase separation and crystal morphology.

2. Experimental

2.1. Materials

The PP, PS and SBS used in the experiment are commercial products, PP (2401, melt flow index is 2.5 g/10 min) and PS (666D, melt flow index is 4.3 g/10 min) were purchased from the Yan Shan Petroleum Chemical, China; SBS (F675, $M_n = 1.8 \times 10^5$, and the styrene content is about 40%) was purchased from the Mao Ming Petroleum Chemical, China.

2.2. Samples preparation

Various blends were prepared by varying the PS content from 0 to 100% (wt%). Melt blending of a pair of polymers was conducted using twin-screw extruder (TSSJ-25 co-rotating twin-screw extruder). After making droplets, the blends were molded by DPIM technology. The schematic representation of this technology is shown in Fig. 1, and the specimen is shown in Fig. 2. The detailed experiment procedure was described in Refs. [32,33]. The DPIM technology relies on the application of shear stress fields to melt/solid interfaces during the packing stage by means of hydraulically actuated pistons. The main feature is that after the melt is injected into the mold the specimen is

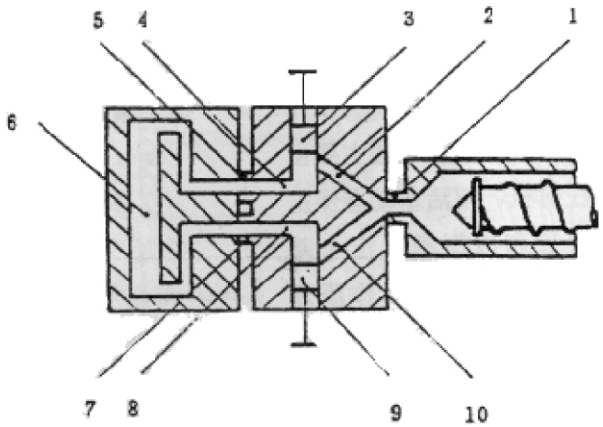

Fig. 1. The schematic representation of DPIM. (1) nozzle, (2) sprue A, (3) piston A, (4) runner A, (5) connector, (6) specimen, (7) connector, (8) runner B, (9) piston B, (10) sprue B.

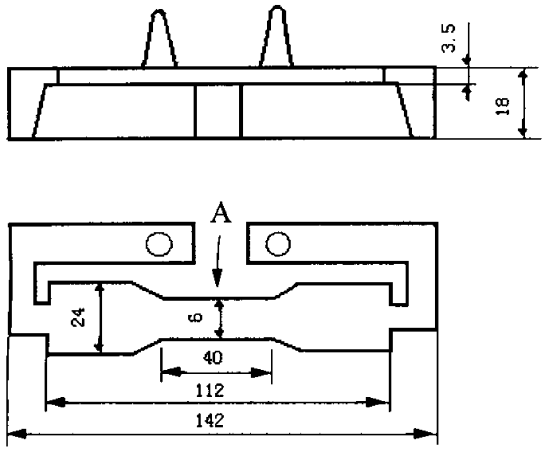

Fig. 2. The sketch of mechanical test specimen dimensions according to ASTM638 M standard.

forced to move repeatedly in a chamber by two pistons that move reversibly with the same frequency as the solidification progressively occurs from the mold wall to the molding core part. The processing parameters are listed in Table 1. We also prepared the 'static' specimens by using the conventional molding technology for comparison purpose. The specimen obtained by DPIM is called dynamic sample, and the specimen obtained by static packing injection molding is called static sample.

2.3. Mechanical properties measurement

RG T-10 Universal Testing Machine was used to measure the stress–strain curves, moving speed was 50 mm/min. the measure temperature was 20 °C. For impact strength measurement, the central part of sample (40 mm long) was used. A notch with 45° was made by machine and remained width is 5.0 mm. The experiment was carried out on an I200XJU-2.75 Impact tester according to ISO 179. The values of all the mechanical parameters are calculated as averages over 6–9 specimens for each composition.

2.4. SEM experiment

The morphologies of the blends were studied by preferential etching of the PS phase in butanone for 2.5 h. The samples were fractured in liquid nitrogen prior to etching. Then the phase morphology was observed in an SEM instrument, JSM-5900LV, operating at 20 KV.

Table 1
Processing parameters in DPIM

Processing parameters	Parameters value
Injection pressure (MPa)	90
Packing pressure (MPa)	50
Melt temperature (°C)	180
Mould temperature (°C)	20
Dynamic packing pressure (MPa)	35
Dynamic packing frequency (Hz)	0.3

3. Results

3.1. PP/PS blends

3.1.1. Mechanical properties

Let's begin with the mechanical properties of PP/PS system first. Fig. 3a shows the typical stress–strain curves of static samples of PP/PS blends. One observes a sharp decrease of elongation at break from 20% of PP to 5% of the blends when adding PS to the PP matrix. This is most likely due to the fact that PP and PS are completely immiscible.

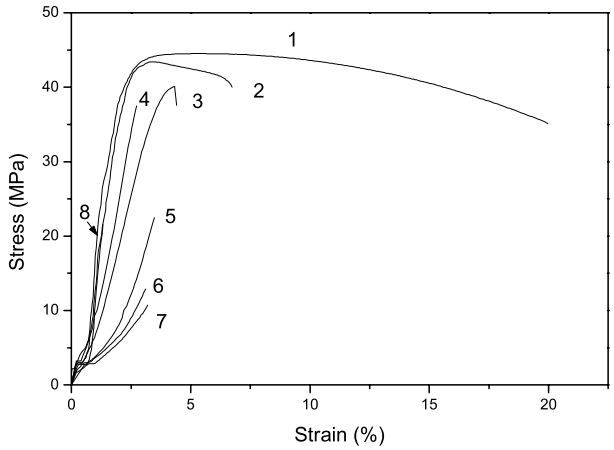

(a)

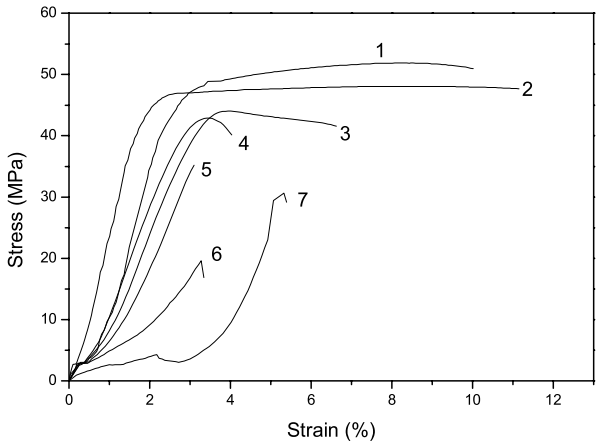

(b)

Fig. 3. The typical stress–strain curves of PP/PS blends, (a) static samples and (b) dynamic samples: PP/PS = (1) 100/0, (2) 90/10, (3) 80/20, (4) 70/30, (5) 50/50, (6) 30/70, (7) 20/80, (8) 10/90.

Not only the elongation, but also the yield stress (tensile strength) decrease as increasing of PS content up to 80 wt%, where a minimum is seen. Then the tensile strength increases again with further increasing of PS content. This result is in a good agreement with that obtained by Xie [7]. For dynamic samples, on the other hand, the decreasing of elongation is more gradually compared with that of pure PP (Fig. 3b). In fact, one even see a slight increase of elongation when 10 wt% of PS is added to PP. In this case, not only the phase morphology, but also the orientation of the components plays an important role to determine the final elongation. As a summary, the tensile strength of samples as function of PS content is shown in Fig. 4. The values are calculated as averages over 6–9 specimens for each composition, and the data for both static and dynamic samples is plotted in one figure for comparison. Two important features should be noted in Fig. 4: (1) the tensile strength of dynamic samples is higher than that of static samples in the whole composition region, due to the molecular orientation induced by shear stress in DPIM. And (2) the minimum occurs at 80 wt% PS content for static samples, but shifts to 70 wt% PS content for dynamic samples, which indicating the phase morphology may be changed under the shear stress. It should be noted that the tensile strength also depends on the direction of measurements, further tensile experiments are needed on samples with different orientation with respect to the tensile direction. This work is undertaking in our group.

The Izod Notched impact strength of the samples was also carried out with the fracture loading perpendicular to the shear flow direction. This is shown in Fig. 5. For static samples, one observes a very low impact strength (4–5 KJ/m^2) for pure PP, and the impact strength keeps constant up to 50% PS content, and down to 1.5 KJ/m^2 at 90 wt% of PS content. For dynamic samples, a very high impact strength (21 KJ/m^2) is seen for pure PP. This is caused by two factors (1) the molecular orientation of PP induced by shear stress and (2) the fracture loading is perpendicular to the shear flow direction. The impact strength of dynamic samples

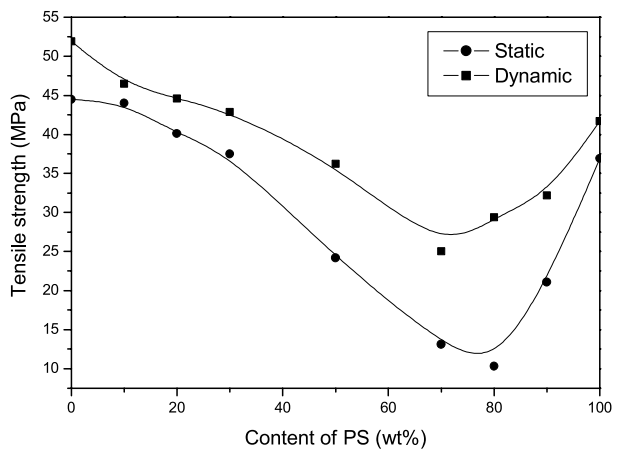

Fig. 4. The tensile strength of PP/PS blend as the function of PS content.

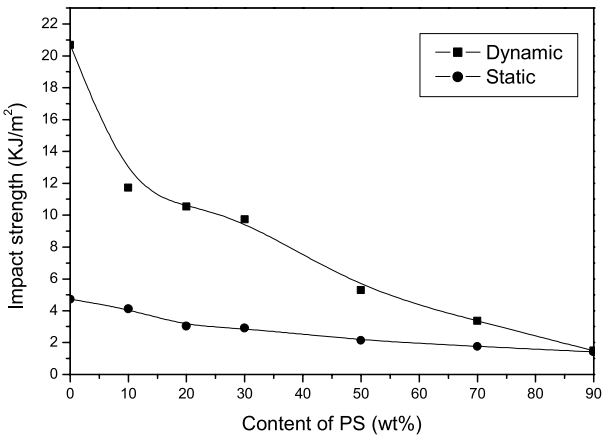

Fig. 5. Impact strength of PP/PS blends as the function of PS content.

decreases sharply from 21 to 12 KJ/m^2 at 10 wt%, 10 KJ/m^2 at 30 wt%, 6 KJ/m^2 at 50%, and down to 2.5 KJ/m^2 at 90 wt% PS content, respectively. Actually, the difference of the impact strength between static and dynamic samples is very little at PS content larger than 50 wt%. This result suggests that, the effect of orientation of PP on impact strength becomes less important as increasing of PS content, and the phase morphology plays a dominating role to determine the impact strength.

3.1.2. Phase morphology

Due to the fast cooling of the melt at the surface of mold, usually the skin and core-like structure is seen on the cross-section area for static samples. The dispersed phase in the core has a bigger size than that in the skin layer, due to the temperature difference in the samples. The core has a higher temperature thus a longer time for phase separation. Fig. 6 is the change of morphology of static samples at central part (the core) as a function of composition. The black domains indicate the position of the extracted PS phase. One observes a sea-island structure in the composition to 50 wt% PS content, which indicates that PS forms a dispersed phase and PP forms a continuous phase in these composition region. The shape of PS dispersed phase is spherical and the size of PS increases from 0.2 to 0.4 to 1–1.5 μm when PS content increases from 10 to 50 wt%. There is a big increase of PS domain size (like a co-continuous structure) at 70 wt% PS content. A clear cut co-continuous morphology is seen at 80 wt% PS content, where the minimum tensile strength is observed in Fig. 4.

In contrast to the static samples, macroscopically the shear-induced morphology of dynamic samples can be divided into three parts instead of two parts. They are the core in the center and oriented zone surrounding the core and the skin layer, as in the case of other polyolefin blends achieved by DPIM. To be compared with Fig. 6, Fig. 7 shows the morphological change as a function of PS content at the center for the dynamic samples. Not very much difference is seen up to 50 wt% PS content, in terms of the particle shape and size. However, one indeed observes a big

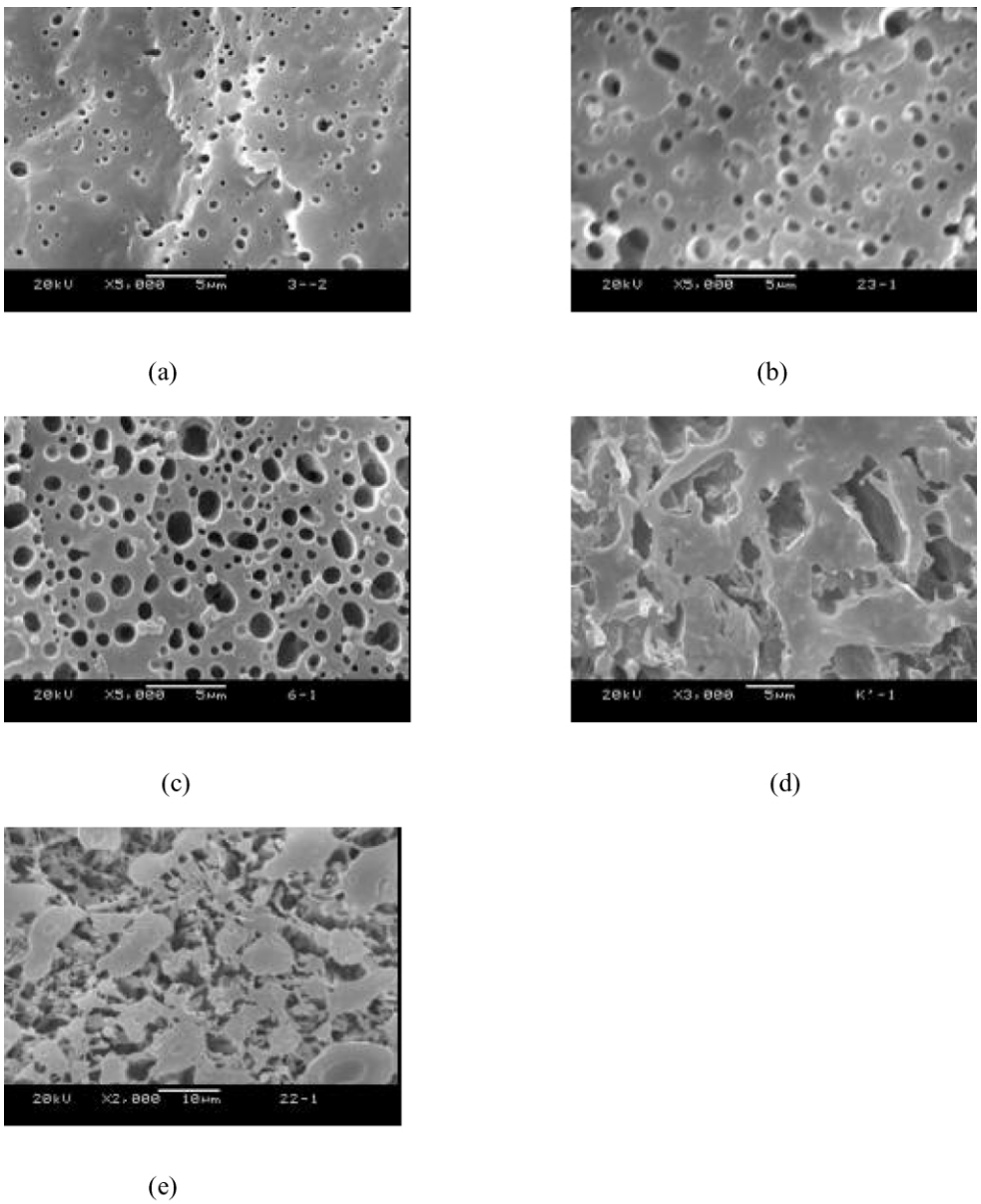

Fig. 6. SEM photographs of PP/PS obtained by static packing injection molding (in the core), PP/PS = (a) 90/10, (b) 70/30, (c) 50/50, (d) 30/70 and (e) 20/80.

change of phase morphology with samples at 70 and 80 wt% PS content. Now the co-continuous structure occurs obviously at 70 wt% PS content (Fig. 7d), where the minimum tensile strength is seen in Fig. 4. PP is found to forms a dispersed phase instead of continuous phase at 80 wt% PS content, as shown in Fig. 7e. To further verify the shear induced morphological change, the phase morphology at the oriented zone, where the effect of shear stress can be most demonstrated, was examined. This is shown in Fig. 8. It can be seen that the morphology is apparent different from the static samples and from the center part of dynamic samples. PS particles are no longer spherical but elongated and deformed seriously. With the increase of PS content, the deformed particles become bigger and coarser. The co-continuous structure is seen even at 30 wt% of PS content (Fig. 8b).

3.2. PP/PS/SBS blends

Not only the composition, but also the interfacial tension plays a role to determine the phase morphology for the immiscible blends. A suitable compatibilizer is often used for improving interfacial adhesion between the components. SBS is frequently selected as the compatibilizer for PP/PS blends [27]. In our work, we also choose SBS as the compatiblizer to investigate the change of mechanical properties as well as morphology under the effect of shear stress. Fig. 9 shows the typical stress–strain curves of PP/PS (70/30) blends as function of SBS content. An increase of elongation is seen for both static and dynamic samples as increasing of SBS content, combined with a decrease of tensile strength. The tensile strength of PP/PS blends with different SBS content is shown in Fig. 10. Fig. 10a shows

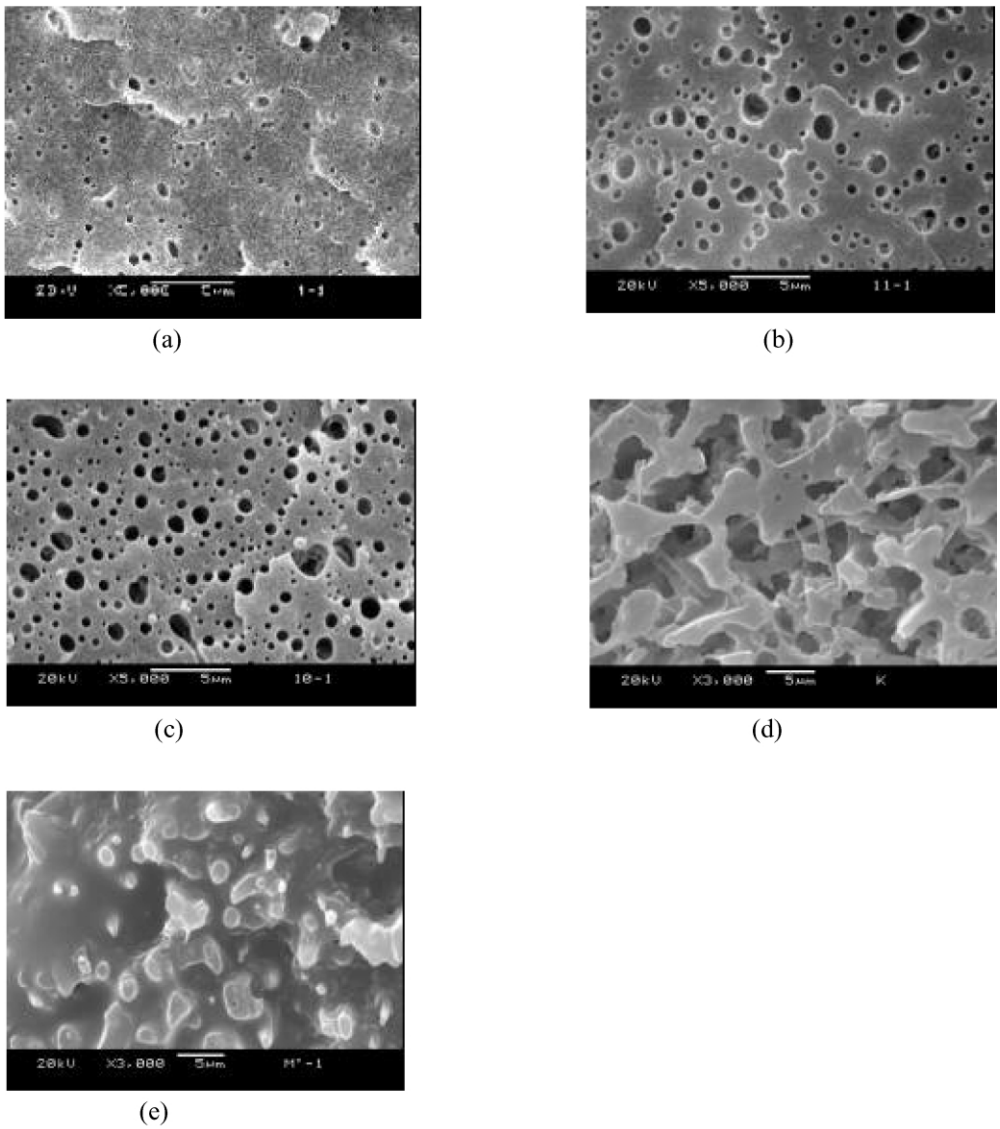

Fig. 7. SEM photograph of PP/PS blends obtained with DPIM (in the core) PP/PS = (a) 90/10, (b) 70/30, (c) 50/50, (d) 30/70 and (e) 20/80.

the result for static samples and Fig. 9b is the tensile strength of dynamic samples. As PS content is low (say less than 30 wt%) the tensile strength decrease as adding of SBS as compatiblizer both for static samples and dynamic samples. In this case, SBS acts as rather a softening-material than as a compatiblizer. The tensile strength is found to increase as increasing of SBS content when PS content is larger than 30 wt% for static samples, or when PS content is larger than 50 wt% for dynamic samples. In this case, the enhancement of interfacial interaction plays a dominating role to determine the tensile strength.

However, the reduced difference among the dynamic samples with different SBS contents seems to suggest that the shear stress will reduce, to certain extent, the effect of SBS on the interface thus tensile strength (Fig. 10b). Actually, shear induced phase separation at low shear rate has been reported [38].

Fig. 11 shows the impact strength with the adding of SBS for both static and dynamic samples. The enhancement of impact strength is observed for all the composition. The trend is more or less the same for both static and dynamic samples. The increasing of impact strength is understood as due to the improvement of interaction between PP and PS when SBS serves as a compatiblizer.

The phase morphologies of PP/PS (70/30) blends with different SBS content are shown in Fig. 12 (center part of static samples) and Fig. 13 (oriented zone of dynamic samples). It is obvious that the size of dispersed PS particles is reduced with adding of the SBS co-polymer both for static and dynamic samples. However, the increasing of SBS content, from 2 to 10 wt%, does not help very much for the further decreasing of the particle size. Not only the decreasing of PS particle size, but also the co-continuous structure (Fig. 13a) at oriented zone is changed into droplet morphology (Fig. 13b–d) with adding of SBS for dynamic samples. At this moment, only the morphology of

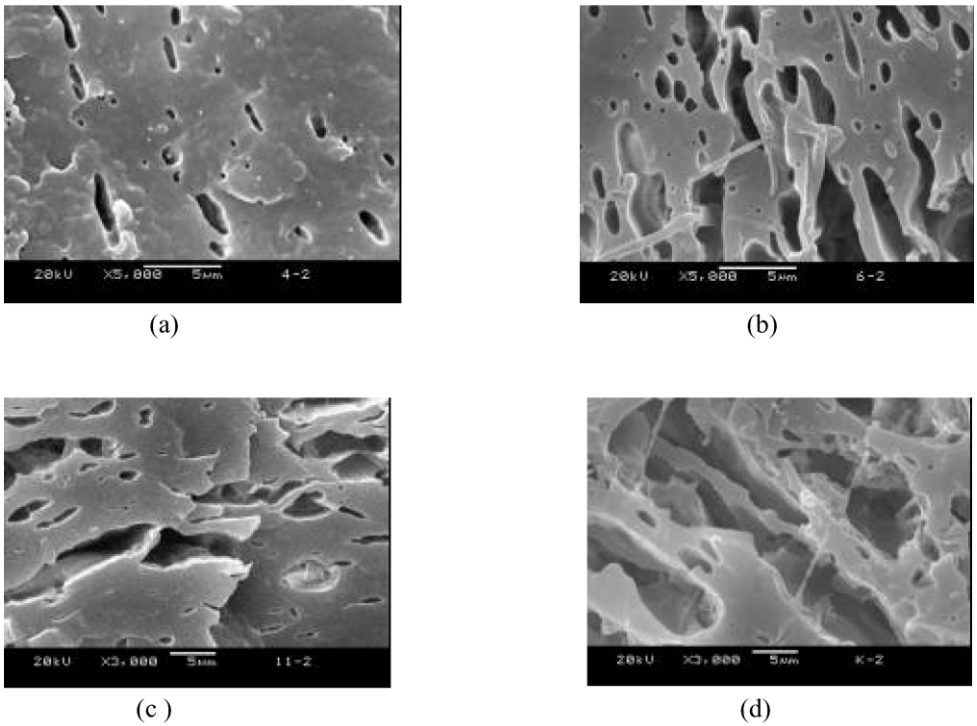

Fig. 8. SEM photograph of PP/PS blends obtained by DPIM (oriented zone) PP/PS = (a) 90/10, (b) 70/30, (c) 50/50 and (d) 30/70.

compatibilized PP/PS (70/30) blends was studied, to show, as an example, the morphological change of the blends before and after DPIM. The interesting concentration region should also cover PS content from 30 to 80 wt%, where the difference between the two preparation methods is remarkable.

4. Discussions

4.1. Region of phase inversion

The phase inversion is a common phenomenon in immiscible polymer blends. Jordhamo et al. [39] developed an empirical model based on the melt-viscosity ratio, η_d/η_m, and the volume fraction ϕ, of each phase for predicting the phase inversion region in immiscible polymer blends. Phase inversion should take place as the following criterion holds:

$$\frac{\eta_1}{\eta_2}\frac{\phi_2}{\phi_1} = 1 \tag{1}$$

Jordhamo's model however, is limited to low shear rates and does not take into account the effect of variations in the interfacial tension between the phases. For the PP/PS blends studied here, both the shear stress and interfacial tension should be considered to explain the observed region of phase inversion. Since the viscosity ratio during processing conditions is not available at moment, one cannot predict the region of phase inversion. For static samples, it should be around 80 wt% PS content from the SEM result (Fig. 6) and correspondingly, one sees the minimum of the tensile strength at 80 wt% PS content (Fig. 4a). For dynamic samples, however, the phase inversion is found to shift 70 wt% PS content at the center part, and a co-continuous phase is observed. This is shown in Fig. 7, which indicating that the region of co-continuity shift towards lower PS content under shear stress field. Correspondingly, the minimum of tensile strength at 70 wt% content is seen (Fig. 4b). At high shear rate zone (oriented zone), the co-continuous structure is seen even at 30 wt% of PS content (Fig. 8b). The effect of shear stress on the region of phase inversion is schematically shown in Fig. 14. Without shear stress, generally speaking, the PS dispersed phase forms spherical in the core layer (center part). However, under shear stress, the PS phase is elongated in sheet-like or ellipsoidal form in the flow direction, and the degree of elongation is different in oriented zone and in the core. At oriented zone, the elongation is strong and becomes weaker in the core. As shown in Fig. 14, phase inversion is expected to occur at lower PS content (30 wt%) in the oriented zone, and at higher PS content (70%) in the core.

4.2. The morphology of polymer blends vs. processing

It is well known that the morphology of polymer blends depends mainly upon the rheological and interfacial properties, the blending conditions, and the volume ratio of the components. The size and the deformation of a purely viscous (Newtonian) droplet surrounded by another Newtonian fluid is determined mainly by two parameters

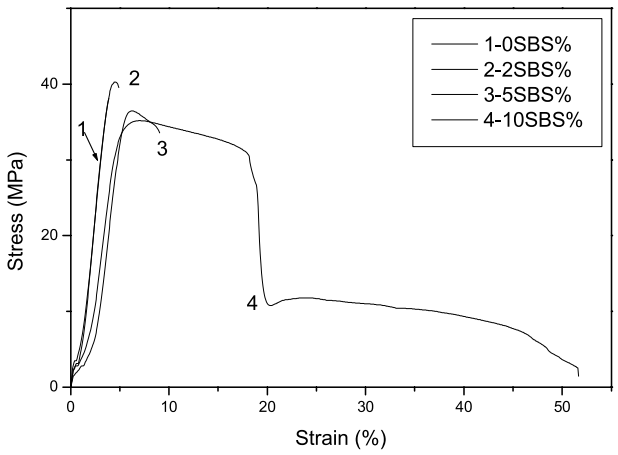

(a)

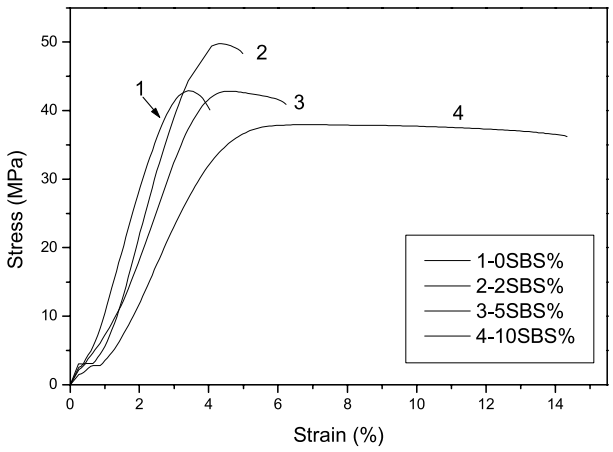

(b)

Fig. 9. The typical stress–strain curves of PP/PS (70/30) blends as function of SBS content, (a) static samples and (b) dynamic samples.

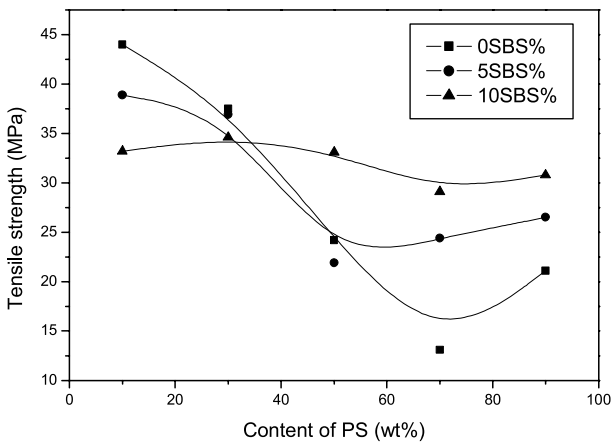

(a)

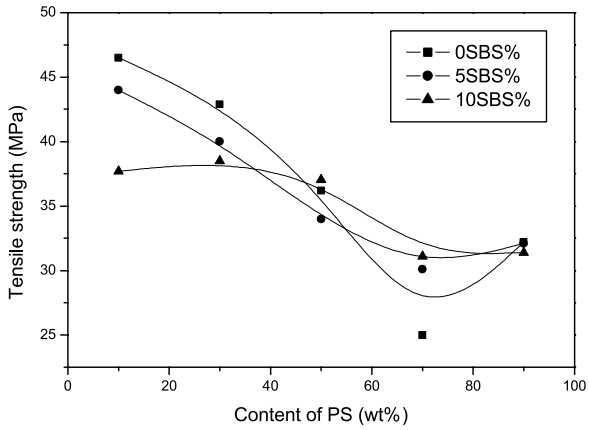

(b)

Fig. 10. The tensile strength of PP/PS blends with different SBS content, (a) static samples and (b) dynamic samples.

[40,41]:

(a) the viscosity ratio (λ):

$$\lambda = \frac{\eta_d}{\eta_m} \tag{2}$$

In the equation, the η_d is the viscosity of dispersed phase and the η_m is the viscosity of matrix.

(b) the k-term of the form

$$k = \frac{\sigma}{\eta_m \cdot \dot{\gamma} R} \tag{3}$$

where σ is interfacial tension, $\dot{\gamma}$ is shear rate, and R is droplet radius. The physical meaning of the k-term is a balance between the resistance to deformation of the droplet (σ/R) and the local acting shear stress ($\eta_m \cdot \dot{\gamma}$) which deforms the droplet. For the polymers of viscoelastic rather than viscous nature, σ in the k-term has to be corrected by a factor that considers the effect of the normal forces arising from the elasticity of the phases [42]. So by choosing the viscosity ratio, controlling the interfacial tension (for example, via using compatiblizer) and shear rate, the phase morphology of polymer blends can be well controlled.

For an injection molded PP/PS blends, the phase morphology is quite complicated. An anisotropy distribution of PS size and shape is evident. As mentioned before, the skin and core-like structure is seen on the cross-section area for static samples, and the morphology of core in the center and oriented zone surrounding the core and the skin layer is observed for dynamic samples.

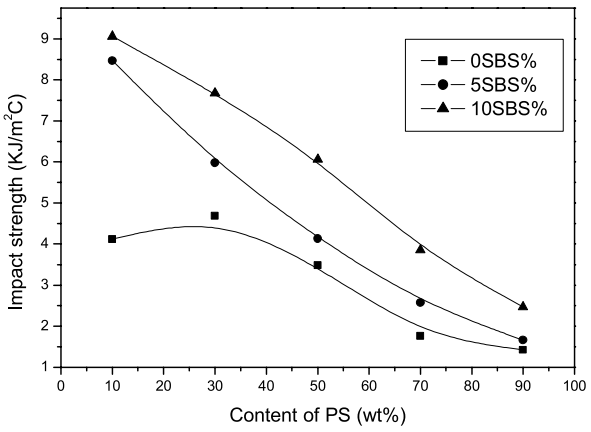

(a)

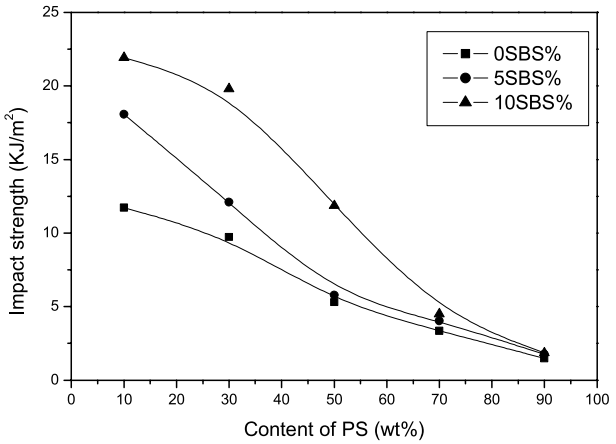

(b)

Fig. 11. The impact strength of PP/PS blends with different SBS content, (a) static samples and (b) dynamic samples.

Even more complicated, as discussed above, for dynamic samples, the co-continuous phase is seen at 30% PS content at oriented zone but 70% PS content at the core. The effect of interfacial tension on the phase morphology is demonstrated in Figs. 12 and 13. The reduced particle size with adding SBS is understood as resulting from the reduced interfacial tension. According to the Eq. (3), the smaller the droplets, the greater is the resistance to deformation. On the other hand, the greater the shear stress, the easier is the deformation. So under the combined effect of shear stress and SBS compatiblizer, not only the decreasing of PS particle size, but also the co-continuous structure (Fig. 13a) at oriented zone is changed into droplet morphology (Fig. 13b–d).

4.3. Tensile modulus

Compared with tensile strength and impact strength, the tensile modulus is frequently used for theoretical prediction. Tensile moduli of polymer blends are strongly dependent on the composition and morphology. In the case of a droplet-matrix morphology the tensile modulus will be largely determined by the modulus of the matrix phase. A relatively high and isotropic value of tensile modulus is expected for co-continuous blends due to their interpenetrating phase structure [43]. It was reported that the modulus of a fibrous blend can be largely determined by modulus of the dispersed (fibrous) phase, especially in oriented samples [44,45]. Theoretically, several models can be found which describe tensile moduli of blends as a function of the composition [46–50]. The moduli of polymer blends generally range between an upper bound, E_u, given by the parallel model [46]:

$$E_u = \Phi_1 E_1 + \Phi_2 E_2 \tag{4}$$

And a lower bound, E_L, given by the series model [47]

$$\frac{1}{E_u} = \frac{\Phi_1}{E_1} + \frac{\Phi_2}{E_2} \tag{5}$$

In which E_i and ϕ_i are the modulus and volume fraction of phase i. It should be noted that the parallel and series models are only valid for simple and idealized structure. For an injection molded PP/PS blends, especially for dynamic samples, the phase morphology is quite complicated, thus complicated moduli are expected. Fig. 15 shows the tensile modulus of PP/PS blends as a function of composition both for static and dynamic samples. For static samples, a synergetic effect is seen up to 20% of PS content, where the blends shows a higher tensile modulus than that of pure PP from additivity of the modulus via parallel model, due partly to the small phase separation (see Fig. 6a). This result is in somewhat agreement with that reported by Guptaand Purwar [51]. However, beyond 20 up to 100 wt% of PS content, the tensile modulus follows the law described by the series model because of the large phase separation in the blends (Fig. 6b–e). An increasing of tensile modulus does not happen when a change of phase morphology from droplet-matrix to co-continuous phase takes place at 80% PS content, as in the case of PE/PS and PE/PP blends as reported by Willemse et al. [42]. For dynamic samples, the orientation of the components plays an important role to determine the tensile modulus, additional to the morphology and composition. Comparing the difference of tensile modulus between dynamic and static samples of pure PP and PS, one observes a big enhancement for PP but a small enhancement for PS through DPIM. This result indicates that PP molecules are much easier to be oriented along the shear flow direction than PS molecules due to the relatively linear structure of PP molecules compared with PS molecules. As increasing of PS content, a decreasing of tensile modulus is seen and a minimum is reached around

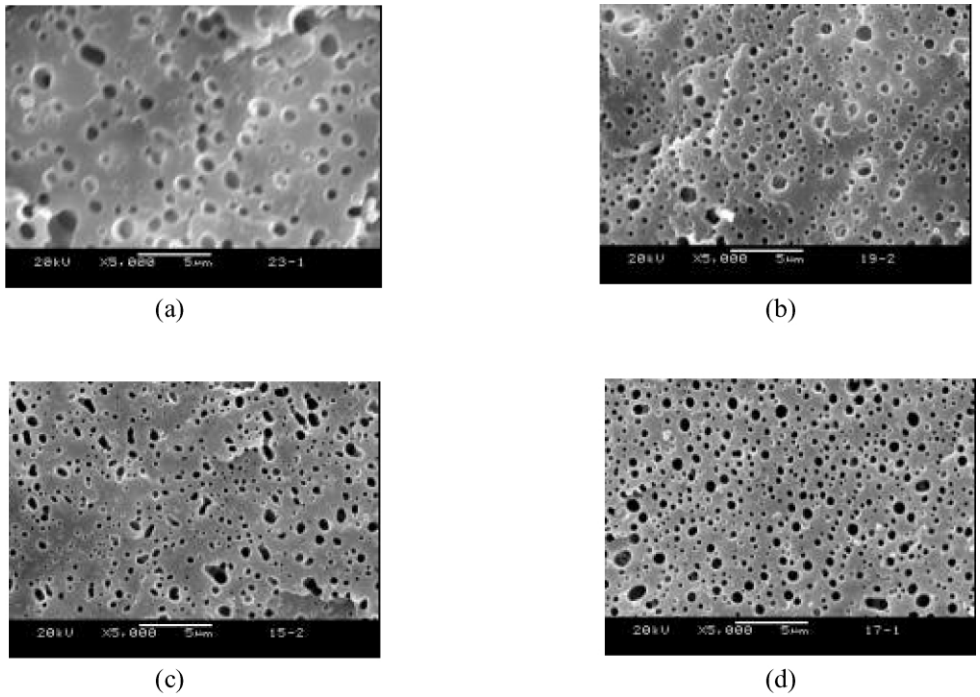

Fig. 12. SEM photograph of PP/PS/SBS blends in the core of static samples, PP/PS/SBS = (a) 70/30/0, (b) 70/28/2, (c) 70/25/5, (d) 70/20/10.

50% PS content. Then tensile modulus increases up to 100 wt% PS content. It should be also noted that the tensile modulus is less than that predicted by the series model in the whole composition region.

A number of factors can be considered to explain the observed decreasing of tensile modulus as increasing of PS content for dynamic samples. It may be due to (1) increasing of phase separation, (2) decreasing of the orientation of PP, this holds especially for composition regions from 30 to 70% PS content, where the co-continuous phase forms either in the oriented zone or the core. Because of the interpenetrating phase networks in co-continuous phase, the molecular orientation will be highly hindered even under shear stress. The combined effect of phase separation and

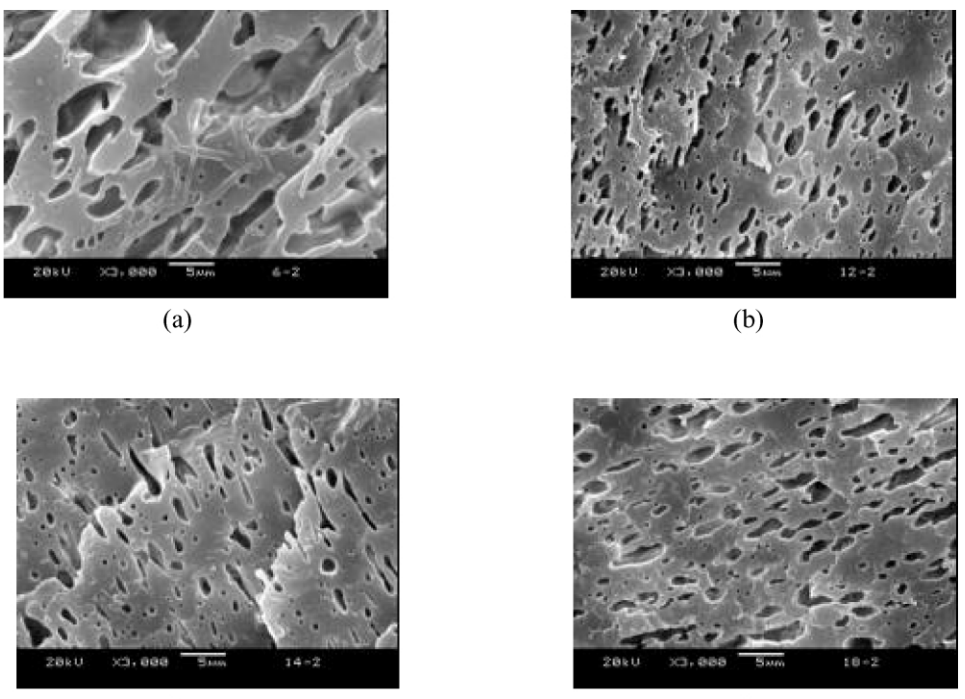

Fig. 13. SEM photograph of PP/PS/SBS blends in the oriented zone of dynamic samples, PP/PS/SBS = (a) 70/30/0, (b) 70/28/2, (c) 70/25/5, (d) 70/20/10.

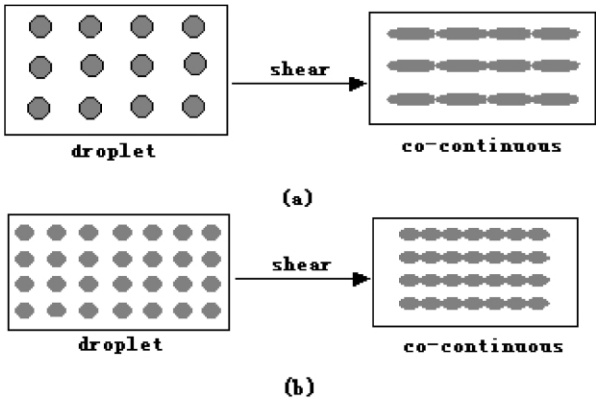

Fig. 14. The schematic representation of morphological change from droplet to co-continuous structure under shear stress, (a) in the oriented zone and (b) in the core.

less oriented molecules causes the minimum of tensile modulus occurs around 50 wt% PS content. Since the tensile modulus is closely related to the molecular orientation, further experiments are needed on samples with different orientation with respect to the tensile direction. This work is undertaking in our group.

5. Conclusion

The shear stress and interfacial tension play an important role to determine the phase morphology thus mechanical properties of PP/PS blends. A complicated morphology with core in the center and oriented zone surrounding the core forms in the cross-section areas of dynamic samples. The phase inversion was also found to occur around 80 wt% PS content for static samples, and shifts towards lower PS content under effect of shear stress, at 70 wt% in the core and 30 wt% in the oriented zone for dynamic samples. The PS particle size is greatly reduced with adding of SBS, and the reduced particle size results in greater resistance to deformation, which causes the co-continuous structure at oriented zone change into droplet morphology. The increasing of phase separation and the decreasing of molecular orientation of PP as increasing of PS content can explain the change of tensile strength and tensile modulus as a function of PS content.

Acknowledgements

We would like to express our great thanks to the China National Distinguished Young Investigator Fund and National Natural Science Foundation of China for Financial Support.

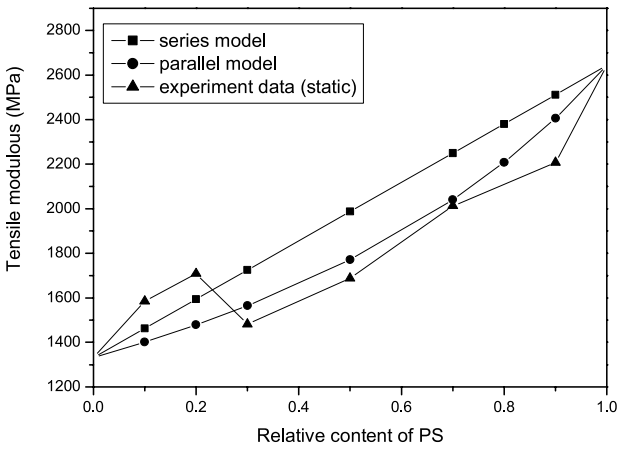

(a)

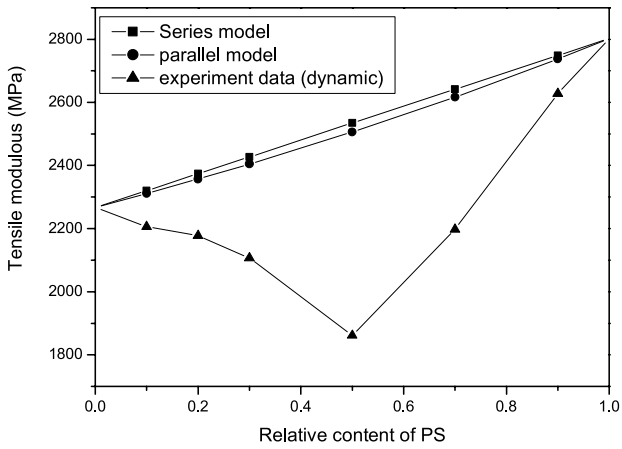

(b)

Fig. 15. The tensile modulus of PP/PS blends as a function of composition, (a) static samples and (b) dynamic samples.

References

[1] Shimizu J, Okui N, Yamamoto T, Ishii M, Takaku A. Sen-I Gakkaishi 1982;38:T-135.
[2] Gupta AK, Purwar SN. J Appl Polym Sci 1985;30:1799.
[3] Iwata I, Yoshimura M, Ishida Y, Tanaka K, Ueki T. Polym Prepr Jpn 1990;39:3599.
[4] Iwata I, Yoshimura M, Ishida Y, Tanaka K, Ueki T. Mech Behav Mater 1992;295.
[5] Cupta VB, Bhuvanesh YC. J Appl Polym Sci 1996;160:1951.
[6] Hlavata D, Horak Z, Lednicky F, Tuzar Z. Polym Networks Blends 1997;7(4):195.
[7] Xie ZM, Sheng J, Wan ZM. J Macromol Sci-Phys 2001;B40(2): 251–61.
[8] Fujiyama M. J Appl Polym Sci 1997;63(8):1015–27.
[9] Lee JK, Han CD. Polymer 1990;40:6277–96.
[10] Lee SG, Lee JH, Choi KY, Rhee JM. Polym Bull 1998;40:765.

[11] Han CD, Kim YW, Chen SJ. J Appl Polym Sci 1975;19:2831.
[12] Han CD. Rheology in polymer processing. New York: Academic Press; 1976. Chapter 7.
[13] Han CD. Multiphase flow in polymer processing. New York: Academic Press; 1981. Chapter 4.
[14] Nelson CJ, Avgeropoulos GN, Weissert FC. Angew Makromol Chem 1977;49:60.
[15] Gaillard P, Ossenbach M, Reiss G. Macromol Chem, Rapid Commun 1980;1:771.
[16] Bartlett DW, Paul DR, Barlow JW. Mod Plast 1981;12:60–3.
[17] Barlow JW, Paul DR. Polym Engng Sci 1984;24:525.
[18] Del Giudice L, Cohen RE, Attalla G. J Appl Polym Sci 1985;30:4305.
[19] Brown HR. Macromolecules 1989;22:2859.
[20] Creton C, Framer EJ, Hadziioannou G. Macromolecules 1991;24: 1846.
[21] Appleby T, Czer F, Moad G, Rizzardo E, Stavropoulos C. Polym Bull 1994;32:479.
[22] Hlavata D, Horak Z. Eur Polym J 1994;30:597.
[23] Horak Z, Fort V, Hlavata D. Polymer 1996;37:65.
[24] Hlavata D, Horak Z, Fort V. Polym Networks Blends 1996;6:15.
[25] Hlavata D, Horak Z. Polym Networks Blends 1997;7:195.
[26] Hlavata D, Horak Z. J Polym Sci Part B: Polym Phys 1999;37(14): 1647–56.
[27] Hlavata D, Horak Z. J Polym Sci Part B: Polym Phys 2001;39: 931–42.
[28] Radonjic G, Musil V, Smit I. J Appl Polym Sci 1998;69(13):2625.
[29] Allen PS, Beivis MJ. UK Patent 2,170,140B, European Patent EPO, 188; 120B1, US Patent, 161(4), 1986; 925.
[30] Guan Q, Shen KZ, Li J, Zhu J. J Appl Polym Sci 1995;55:1797.
[31] Kalay G, Bevis M. J Polym Sci, Polym Phys 1997;35:241.
[32] Wang Y, Zou H, Fu Q. J Appl Polym Sci 2002;85:236.
[33] Zhang G, Fu Q. J Appl Polym Sci 2002;86:58.
[34] Fu Q, Wang Y, Li QJ, Zhang G. Macromol Mater Engng 2002;287: 391.
[35] Wang Y, Fu Q, Li QJ, Zhang G. J Polym Sci, Part B: Polym Phys 2002;40:2086.
[36] Na B, Zhang Q, Fu Q. Polymer 2002;43:7367.
[37] Zhang Q, Wang Y, Fu Q. J Polym Sci, Part B: Polym Phys 2003;41: 10.
[38] Hindawi IA, Higgins JS, Weiss RA. Polymer 1992;33:2522.
[39] Jordhamo G, Manson J, Sperling L. Polym Engng Sci 1986;26:517.
[40] Plochocki AP. Polym Engng Sci 1983;23:618.
[41] Berger W, Kammer HW, Kummerlowe C. Makromol Chem Suppl 1984;8:101.
[42] Van OH. J Coll Interf Sci 1972;40:448.
[43] Willemse RC, Speijer A, Langeraar AE. Polymer 1999;40:6645–50.
[44] Machiels AGC, Denys KFJ, Van DJ, Posthuma de BA. Polym Engng Sci 1996;36:2451.
[45] Grevecoeur G. PhD thesis. Belgium: Katholieke Uneversiteit Leuven; 1991.
[46] Nielsen LE. Mechanical properties of polymers and composites, II. New York: Marcel Dekker; 1974.
[47] Halpin JC, Kardos JL. Polym Engng Sci 1976;16:344.
[48] Lees JK. Polym Engng Sci 1968;8:186.
[49] Davies WEA. J Phys D, Appl Phys 1971;4:1325.
[50] Coran AY, Patel R. J Appl Polym Sci 1976;20:3005.
[51] Gupta AK, Purwar SN. J Appl Polym Sci 1985;30:1799.